



**International Journal of Biology, Pharmacy
and Allied Sciences (IJBPAS)**

'A Bridge Between Laboratory and Reader'

www.jbpas.com

NOVEL TETRAHYDRO ISOQUINOLINE ALKALOID DERIVATIVE IN TREATMENT OF COVID 19 BY *INSILICO* STUDIES

HEMALATHA C.N*, HEMAMALINI. B, KEERTHANA.V, MEHUR NISHA.K, PUSHPA
PRIYA.G, SUPRIYA. S AND HARIKRISHNAN.N

Faculty of Pharmacy, Dr.M.G.R. Educational and Research Institute, Velappanchavadi, Chennai-
600 077, Tamil Nadu, India

*Corresponding Author: Dr. Hemalatha C.N: E Mail: hemalatha.pharm@drmgrdu.ac.in

Received 16th June 2020; Revised 24th July 2020; Accepted 29th Nov. 2021; Available online 1st July 2022

<https://doi.org/10.31032/IJBPAS/2021/11.7.6247>

ABSTRACT

Objective: Tetrahydroisoquinoline alkaloid derivative is a nicotinic neurotransmitter receptor antagonist [1] that has been isolated from a spread of plant sources together with sacred lotus. Dimerization results in the biscochlorine alkaloids like cepharanthine and many other phytoconstituents like quercetin, Luteolin, kaempferol etc. [2]. Coclorine mechanism of action states that, Coclorine N-methyltransferase (CNMT) is a key enzyme in the pathway to (S)-reticulene, installing the N-methyl substituent that is essential for the bioactivity of many BIAs (Benzylisoquinoline Alkaloids) [3]. From the literature review we have been examined that there are no recent studies on regards with treatment for COVID 19 with the tetrahydroisoquinoline alkaloid from sacred lotus.

METHODOLOGY: The aim of the study was to investigate the binding efficiency of selected currently COVID 19 treating synthetic drugs, and compared with the plant constituents. The target selected for the study were extracted from Protein Data Bank, and the ligands were extracted from Pubchem. The compounds were screened and shown great binding energy.

Keywords: Tetrahydroisoquinoline, Alkaloid Derivative, COVID 19, *Insilico* studies

INTRODUCTION:

The ongoing pandemic of intense acute respiration syndrome corona virus 2 (SARS-CoV-2) infections has caused greater than 4692797 instances and 195920 deaths globally as of April 25, 2020.¹ Although maximum infections are self-limited, approximately 15% of inflamed adults broaden intense pneumonia that calls for treatment with supplemental oxygen and an extra 5% development to crucial infection with hypoxemic respiration failure, acute respiration syndrome, and multiorgan failure that necessitates ventilatory support, regularly for several weeks. Majorly 1/4th of people suffering from corona virus ailment 2019 (COVID-19) requiring invasive mechanical air flow have died in hospital. Four, five and the related burden on health-care systems, particularly in depth care units, have been overwhelming in numerous affected countries. Although numerous accredited tablets and investigational agents have proven antiviral pastime in opposition to SARS-CoV-2 *in vitro*, At present there aren't any antiviral healing procedures of validated effectiveness in treating significantly ill suffers with COVID-19 [4].

MECHANISM OF ACTION (MOA) of COVID 19:

- ✚ SARS Cov-2 where it is structurally a spike protein composed of RNA which enters into the target cells by endosomal pathway to the cellular receptor angiotensin converting enzyme Angiotensin Converting Enzyme (**ACE-2**).
- ✚ Then the virus which entered in the host cell gets translocated in the endosomal region where on further it gets cleaved by endosomal acid cleavage enzyme and permeates membrane fusion.
- ✚ Translation process occurs and virus starts replicating and releases polyproteins such as **PP1a and PP1ab**. (Protein Phosphatase)
- ✚ Sub-genomic templates for mRNA synthesis and translation of the viral structural proteins arise through discontinuous transcription. Viral genome replication is mediated via way of means of the viral replication
- ✚ Viral nucleocapsids are assembled from the packaged viral genomes and translated viral structural proteins. Infectious virions are then launched through exocytosis [5, 6].

MATERIALS AND METHODS:

Data set:

The ligands were drawn from using RCSB data bank. Some of the molecular structures of reported compounds were drawn in *ChemDraw Ultra software 12.0*. The structures are converted from two-dimensional [2D] to three dimensional [3D] and saved as.pdb format.

Preparation of ligand structure:

The ligand structures of the data set were prepared by LigPrep module of *Schrodinger v11.5*. To give the best results, the structures that are docked must be good representations of the actual ligand structures as they would appear in a protein–ligand complex. This means that for Glide docking the structure must meet the following conditions. They must be three-dimensional (3D) form. Glide only modifies the torsional internal coordinates of the ligand during docking, so the rest of the geometric parameters must be optimized beforehand. They must each consist of a single molecule that has no covalent bonds to the receptor, with no accompanying fragments, such as counter ions and solvent molecules. They must have all their hydrogen (filled valences). They must have an appropriate protonation state for physiological pH values [7, 8].

Preparation of protein structure:

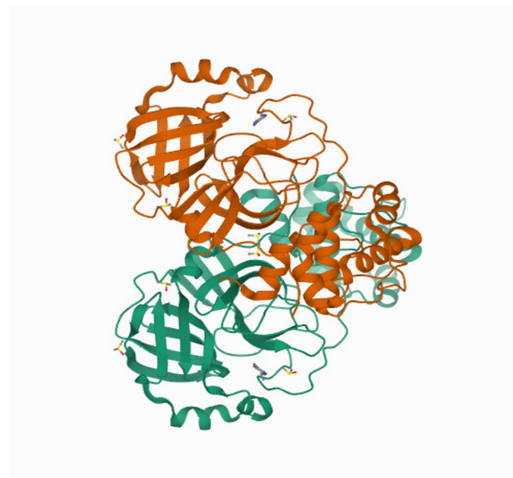


Figure 1- PDB-5482

The selected proteins i.e. (Figure 1: PDB code: 5R82) is obtained from the protein data bank (PDB)

(<http://www.rcsb.org/pdb/home/home.do>).

The imported typical structure file of protein from the protein data bank is not suitable for immediate use to carry out the molecular docking study. A typical PDB structure file consists of heavy atoms and may include a co-crystallized ligand, water molecules, metal ions and cofactors. The ligand and ligand-receptor complex is suitable for use with other Schrödinger modules. The protein structure was prepared using the protein preparation wizard (preprocessed, optimized and minimized) in the *Schrodinger* software graphical user interface *Maestro v11.5* [9].

Preparation of grid

Grid generation is done using receptor grid generation module of *maestro version 11.5*. A grid is generated around the binding site already occupied by the co-

crystallized ligand so that co-crystallized ligand can be excluded and new compounds can be attached to the same bindingsite [10].

Docking:

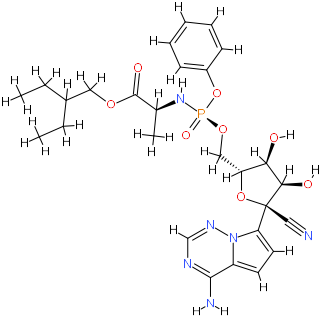
Molecular docking study was applied to investigate the binding mode of compound with selected PDB ID (5R82). Docking score obtained from GLIDE (*maestro v11.5*) and binding site was targeted and the grid was created. The active site grid covered the important amino acids interacting with receptor. The 3D structure of the protein was obtained from protein data bank using their specific (PDB code: 5R82). A data set of currently marketed COVID 19 synthetic and novel plant phytoconstituents of ligands

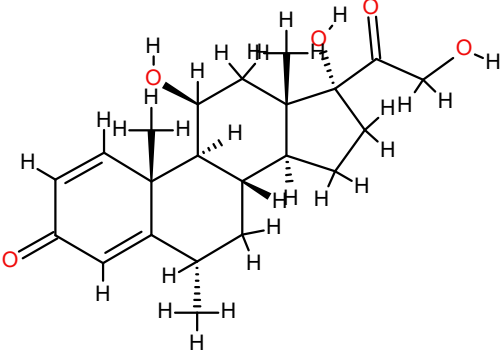
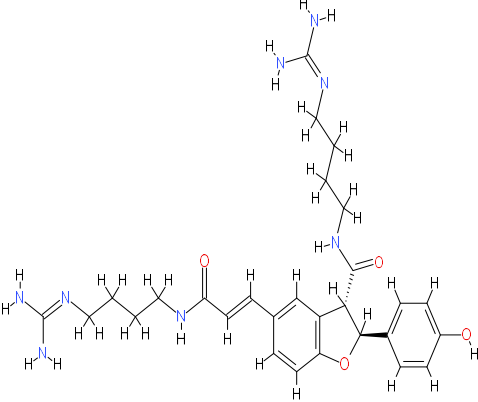
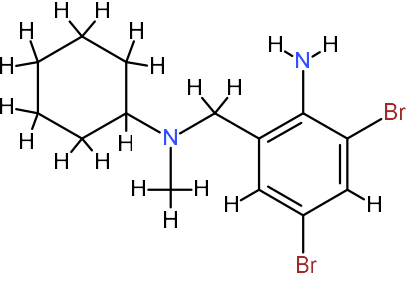
(Table 1 & Table 2) and their structures were drawn using the workspace of Maestro and were converted to 3D form for the docking studies. The collected ligands were prepared for docking. Then the prepared ligands were docked into the generated grid in the prepared protein. The best docked pose with lowest glide score value was recorded for each ligand using *Schrödinger-maestro v11.5 (2018-1)* [11-13].

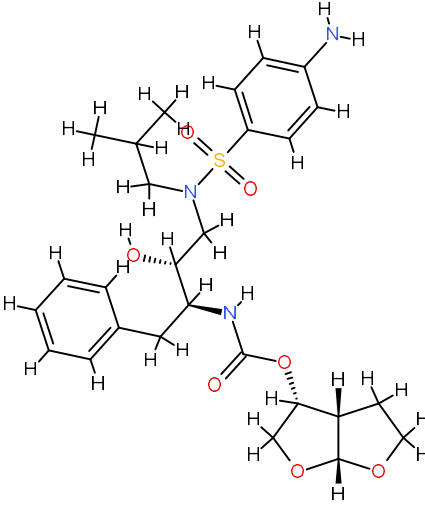
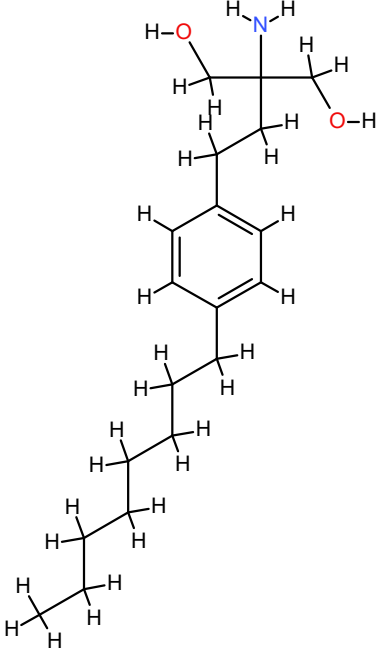
SYNTHETIC DRUGS / MARKETED DRUGS CURRENTLY USED IN COVID 19 (Table 1)

NATURAL SOURCE OF PLANTS DERIVED PHYTOCONSTITUENTS (Table 2)

Table 1: Depicting the structure of compounds (R1-R11) with its molecular weight are depicted below

S. No.	COMMON NAME / IUPAC NAME	STRUCTURE	MOLECULAR WEIGHT
R1	Remdesivir		602.6 g/mol

		 <p>The chemical structure of Hordatine is a complex polycyclic molecule. It features a central six-membered ring fused to a five-membered ring, which is further fused to a six-membered ring. The structure includes several hydroxyl groups (red oxygen atoms) and a carboxylic acid group (red oxygen atoms). The molecule is highly branched and contains multiple stereocenters.</p>	
R6	Hordatine	 <p>The chemical structure of Bromhexine is a complex molecule. It features a central six-membered ring fused to a five-membered ring, which is further fused to a six-membered ring. The structure includes several hydroxyl groups (red oxygen atoms) and a carboxylic acid group (red oxygen atoms). The molecule is highly branched and contains multiple stereocenters.</p>	580.7 g/mol
R7	Bromhexine	 <p>The chemical structure of Bromhexine is a complex molecule. It features a central six-membered ring fused to a five-membered ring, which is further fused to a six-membered ring. The structure includes several hydroxyl groups (red oxygen atoms) and a carboxylic acid group (red oxygen atoms). The molecule is highly branched and contains multiple stereocenters.</p>	412.59 g/mol

R8	Darunavir	 <p>The image shows the chemical structure of Darunavir, a second-generation protease inhibitor. It features a central pyridine ring substituted with a methylamino group, a methyl group, and a propyl chain. The propyl chain is further substituted with a methyl group and a dihydroxyethyl side chain. The dihydroxyethyl side chain is linked to a propanoic acid moiety, which is esterified to a ribose sugar. The ribose sugar is in its cyclic form, with the ester group attached to the C2' position. The structure is drawn with explicit hydrogen atoms and stereochemistry.</p>	593.7 g/mol
R9	Fingolimod	 <p>The image shows the chemical structure of Fingolimod, a sphingosine derivative used in the treatment of multiple sclerosis. It consists of a sphingosine backbone with a hydroxyl group at the C1' position, a methyl group at the C2' position, and a long hydrocarbon chain at the C3' position. The sphingosine backbone is drawn with explicit hydrogen atoms and stereochemistry.</p>	343.9 g/mol

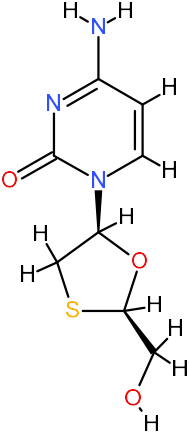
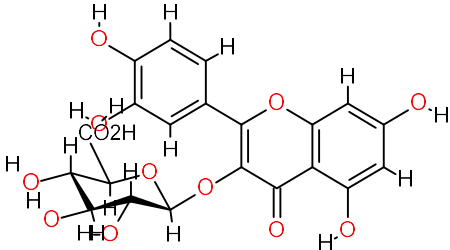
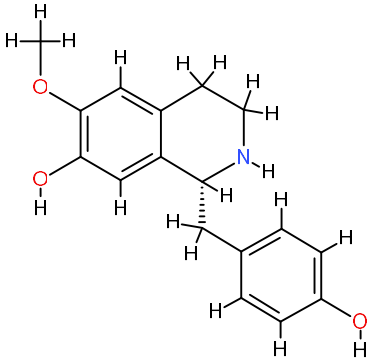
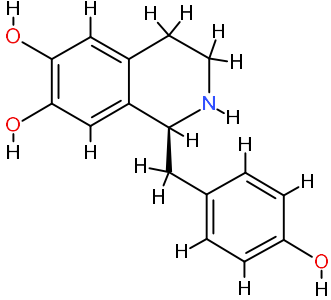
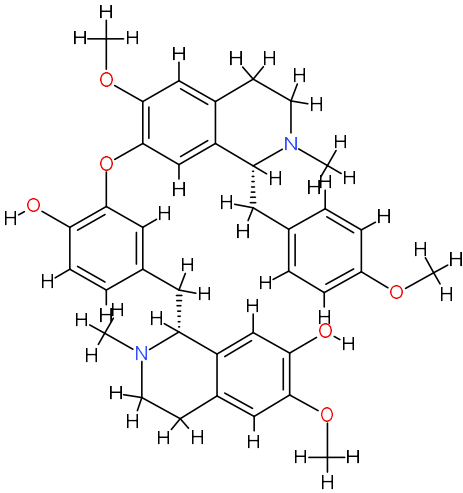
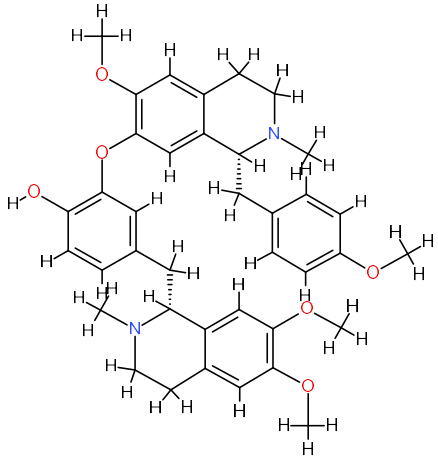
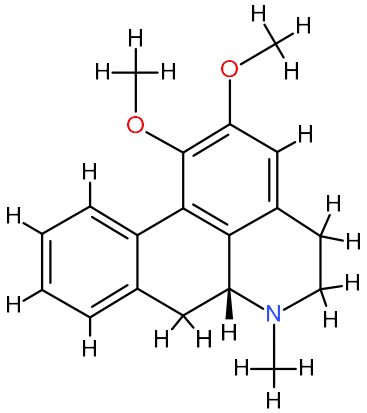
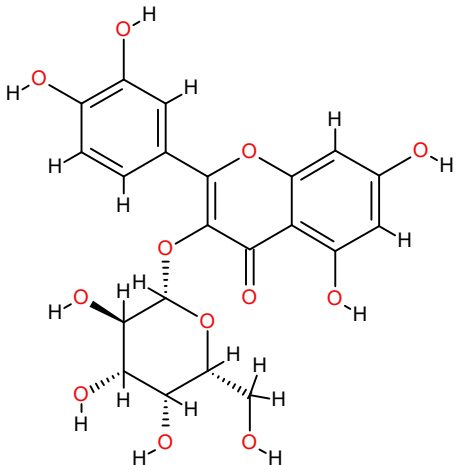
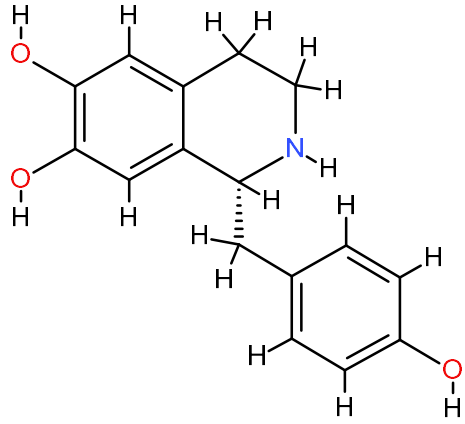
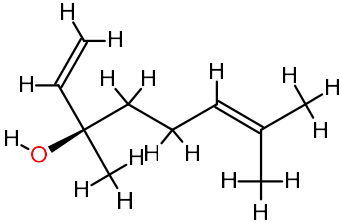
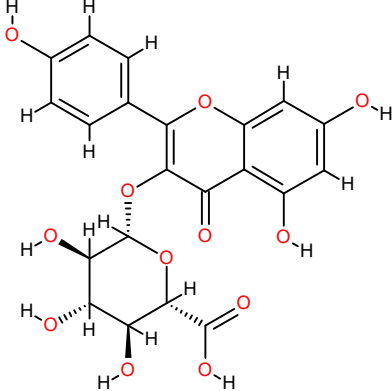
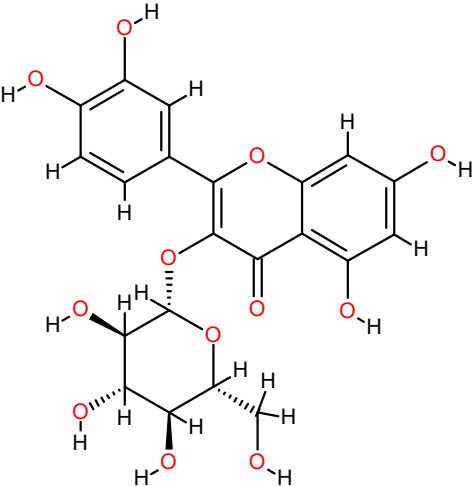
R10	Lamivudine	 <p>The image shows the chemical structure of Lamivudine. It consists of a pyrimidine ring system with an amino group (-NH₂) at the 4-position and a carbonyl group (=O) at the 2-position. The 5-position of the pyrimidine ring is linked to a thiazolidine ring system. The thiazolidine ring has a sulfur atom at the 4-position and a hydroxyl group (-OH) at the 3-position. The 2-position of the thiazolidine ring is attached to a methyl group (-CH₃).</p>	229.26 g/mol
-----	------------	---	--------------

Table 2: Depicting the structure of compounds (P1-P13) with its molecular weight are depicted below

S. No.	STRUCTURE	COMMON NAME/ IUPAC NAME	MOLECULAR WEIGHT
P1	Quercetin 3-O- β -glucouronide	AND Enantiomer  <p>The image shows the chemical structure of Quercetin 3-O-β-glucouronide. It features a central flavone core (quercetin) with a glucose molecule attached to the 3-position of the flavone ring via a glycosidic bond. The glucose is in its cyclic β-D-glucopyranose form. The quercetin core has hydroxyl groups at the 2, 3, 7, and 8 positions.</p>	478.4 g/mol
P2	couclaurine	 <p>The image shows the chemical structure of couclaurine. It consists of a coumarin core with a 7-hydroxy group and a 4-hydroxy group. The 3-position of the coumarin ring is linked to a piperazine ring system. The piperazine ring has a methyl group (-CH₃) at the 2-position and a hydroxyl group (-OH) at the 4-position.</p>	285.34 g/mol

P3	Norcularine	 <p>The chemical structure of Norcularine is a dimeric alkaloid. It consists of two 1,2,3,4-tetrahydroquinoline rings linked at their 2-positions. Each ring is substituted at the 6-position with a 3,4,5-trihydroxyphenyl group. The stereochemistry at the 2-position is (1R,2S).</p>	271.31 g/mol
P4	Isoliensinine	 <p>The chemical structure of Isoliensinine is a complex pentacyclic alkaloid. It features a central 1,2,3,4-tetrahydroquinoline ring system. This core is substituted with two 3,4,5-trihydroxyphenyl groups and two methoxy groups (-OCH₃). The stereochemistry is (1R,2S,3R,4R).</p>	610.7 g/mol
P5	Neferine	 <p>The chemical structure of Neferine is a complex pentacyclic alkaloid, very similar to Isoliensinine. It features a central 1,2,3,4-tetrahydroquinoline ring system substituted with two 3,4,5-trihydroxyphenyl groups and two methoxy groups (-OCH₃). The stereochemistry is (1R,2S,3R,4R).</p>	167.2 g/mol

P6	Nuciferine	 <p>The chemical structure of Nuciferine is a complex polycyclic alkaloid. It features a central hexahydroindole ring system fused to a benzene ring and a pyridine ring. The pyridine ring is substituted with a methyl group and a methoxy group. The benzene ring is substituted with a methyl group and a methoxy group. The hexahydroindole ring is substituted with a methyl group and a methoxy group. The structure is shown in a 3D perspective view with hydrogen atoms explicitly drawn.</p>	295.3755
P7	Hyperin	 <p>The chemical structure of Hyperin is a complex polycyclic alkaloid. It features a central hexahydroindole ring system fused to a benzene ring and a pyridine ring. The pyridine ring is substituted with a methyl group and a methoxy group. The benzene ring is substituted with a methyl group and a methoxy group. The hexahydroindole ring is substituted with a methyl group and a methoxy group. The structure is shown in a 3D perspective view with hydrogen atoms explicitly drawn.</p>	464.4 g/mol
P8	Demethylcoclaurine	 <p>The chemical structure of Demethylcoclaurine is a complex polycyclic alkaloid. It features a central hexahydroindole ring system fused to a benzene ring and a pyridine ring. The pyridine ring is substituted with a methyl group and a methoxy group. The benzene ring is substituted with a methyl group and a methoxy group. The hexahydroindole ring is substituted with a methyl group and a methoxy group. The structure is shown in a 3D perspective view with hydrogen atoms explicitly drawn.</p>	271.31g/mol

P9	Linalool	 <p>The chemical structure of Linalool is shown, featuring a branched carbon chain with two double bonds and a hydroxyl group. The hydroxyl group is attached to a tertiary carbon atom. The structure is drawn in a perspective view with wedges and dashes to indicate stereochemistry.</p>	154.25 g/mol
P10	Kaempferol-3-O-βD-glucuronide	 <p>The chemical structure of Kaempferol-3-O-βD-glucuronide is shown. It consists of a kaempferol aglycone (a flavone with hydroxyl groups at positions 5, 7, and 8) linked to a β-D-glucopyranose sugar at the 3-position. The sugar is shown in its cyclic form with hydroxyl groups at various positions.</p>	462.4 g/mol
P11	Isoquercetin	 <p>The chemical structure of Isoquercetin is shown. It consists of a quercetin aglycone (a flavone with hydroxyl groups at positions 5, 7, and 8) linked to a β-D-glucopyranose sugar at the 3-position. The sugar is shown in its cyclic form with hydroxyl groups at various positions.</p>	464.4 g/mol

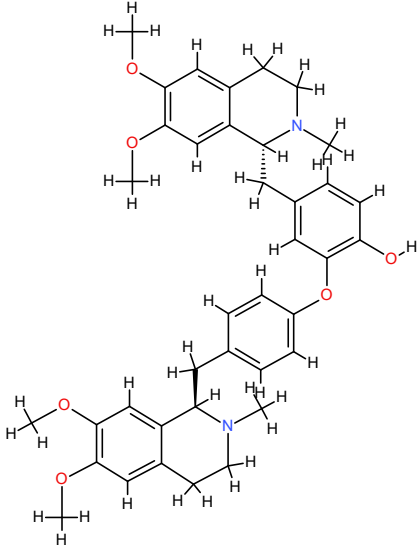
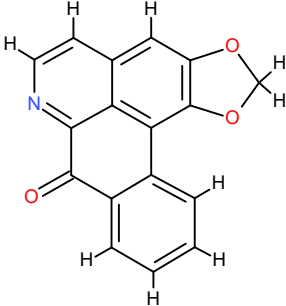
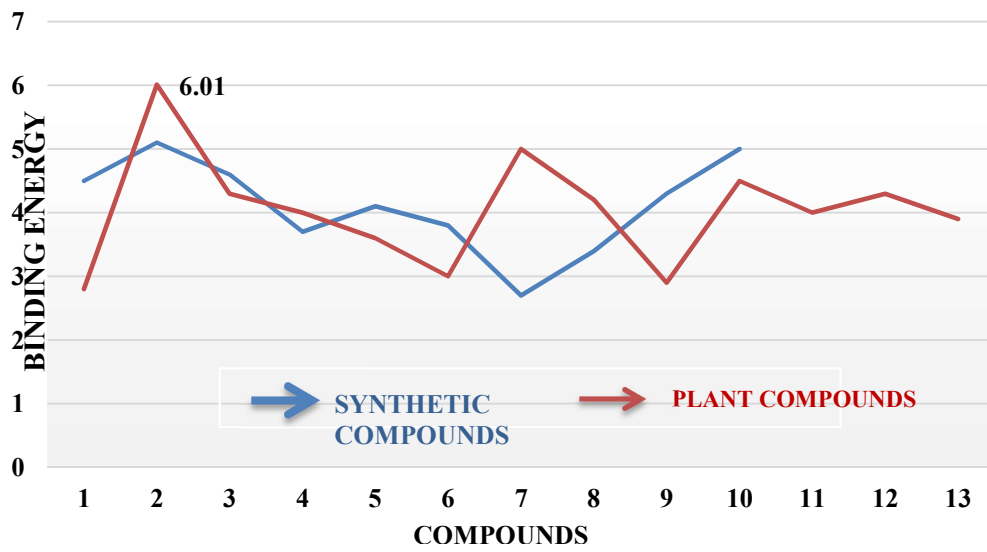
P12	Dauricine		624.8 g/mol
P13	Liriodenine		275.26 g/mol

Table 3: Docking Results For Compounds With Protein For Synthetic Drugs

COMPOUNDS	R1	R2	R3	R4	R5	R6	R7	R8	R9	R10
BINDING ENERGY (Kcal/mol)	-4.56	-5.11	-4.616	-3.722	-4.168	-3.898	-2.791	-3.461	-4.323	-5.073
GLIDE ENERGY (Kcal/mol)	-43.52	-49.264	-29.11	-27.522	-25.91	-38.09	-20.695	-38.996	-34.963	-31.379

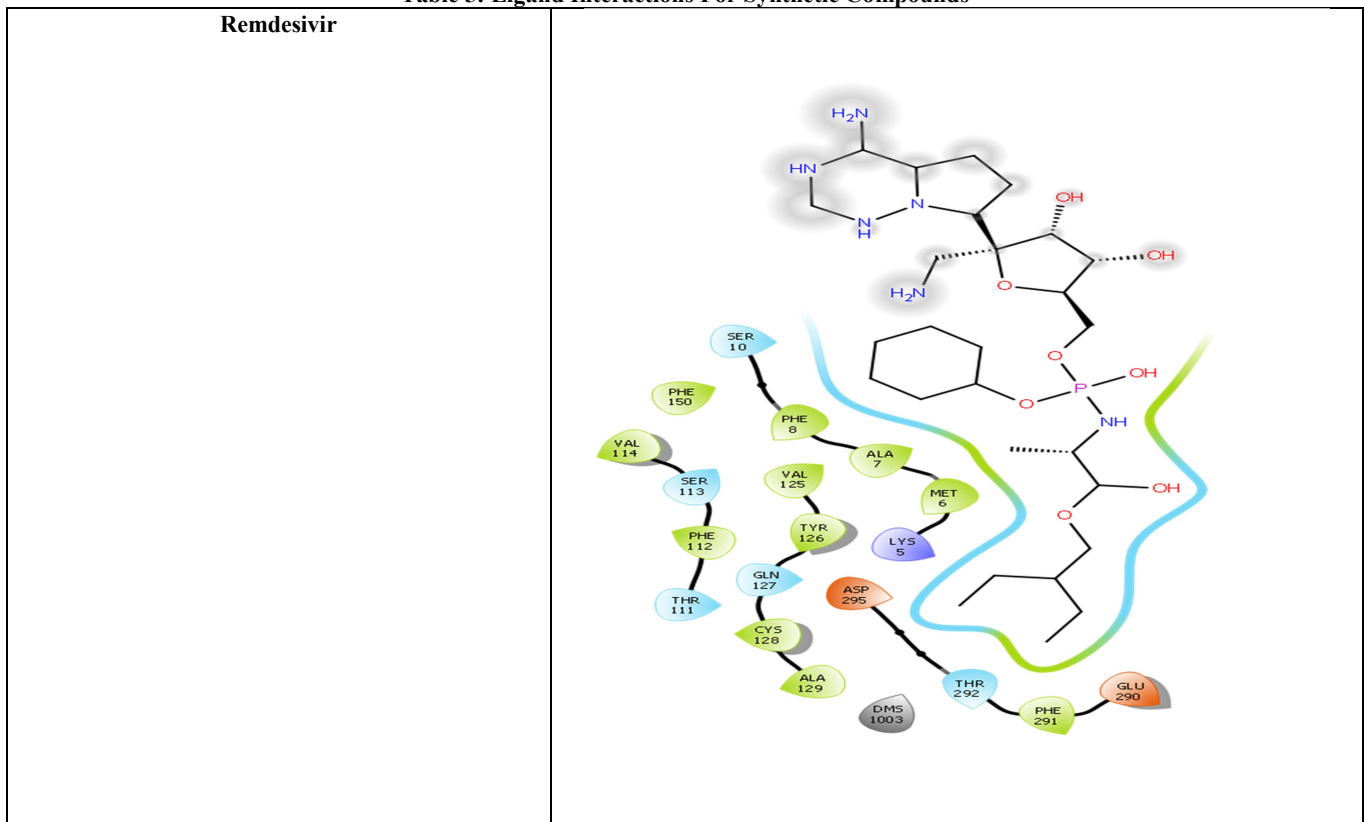
Table 4: Docking Results For Compounds With Protein For Plant Drugs

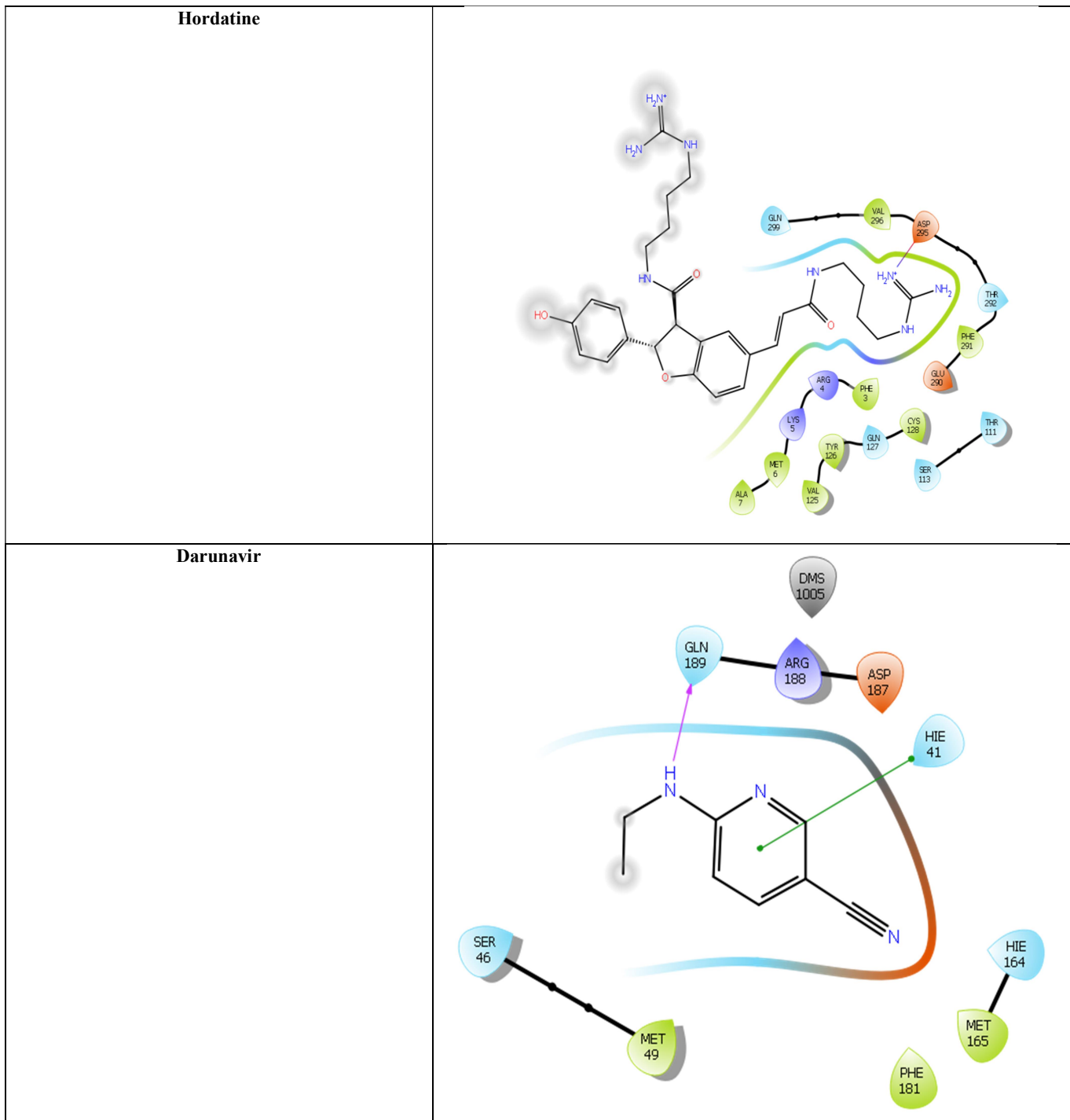
COMPOUNDS	P1	P2	P3	P4	P5	P6	P7	P8	P9	P10	P11	P12	P13
BINDING ENERGY (Kcal/mol)	-2.813	-6.01	-4.34	-4.024	-3.629	-3.008	-5.093	-4.245	-2.953	-4.55	-4.02	-4.323	-3.985
GLIDE ENERGY (Kcal/mol)	-33.58	-38.883	-31.57	-20.97	-26.22	-22.69	-42.88	-44.086	-18.04	-41.16	-21.45	-46.18	-21.01



Graph 1: Comparison of Binding energy of synthetic and Plant compounds

Table 5: Ligand Interactions For Synthetic Compounds





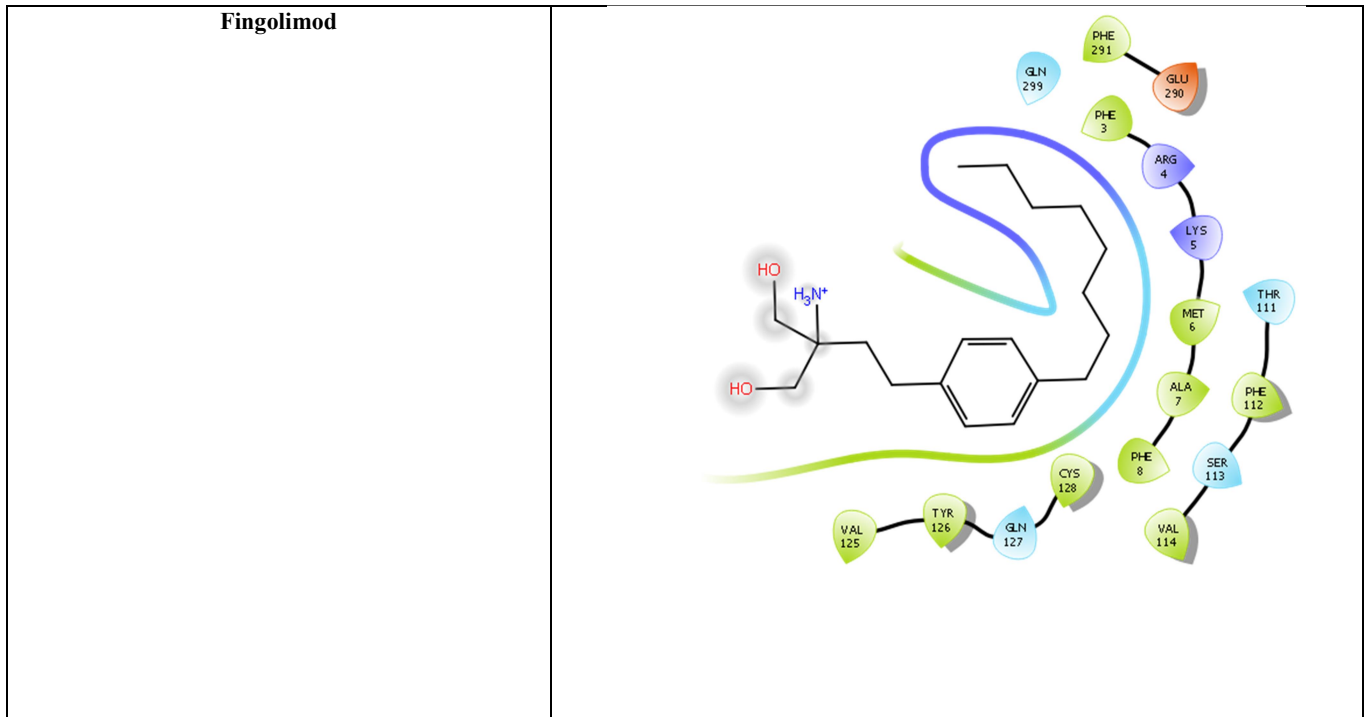
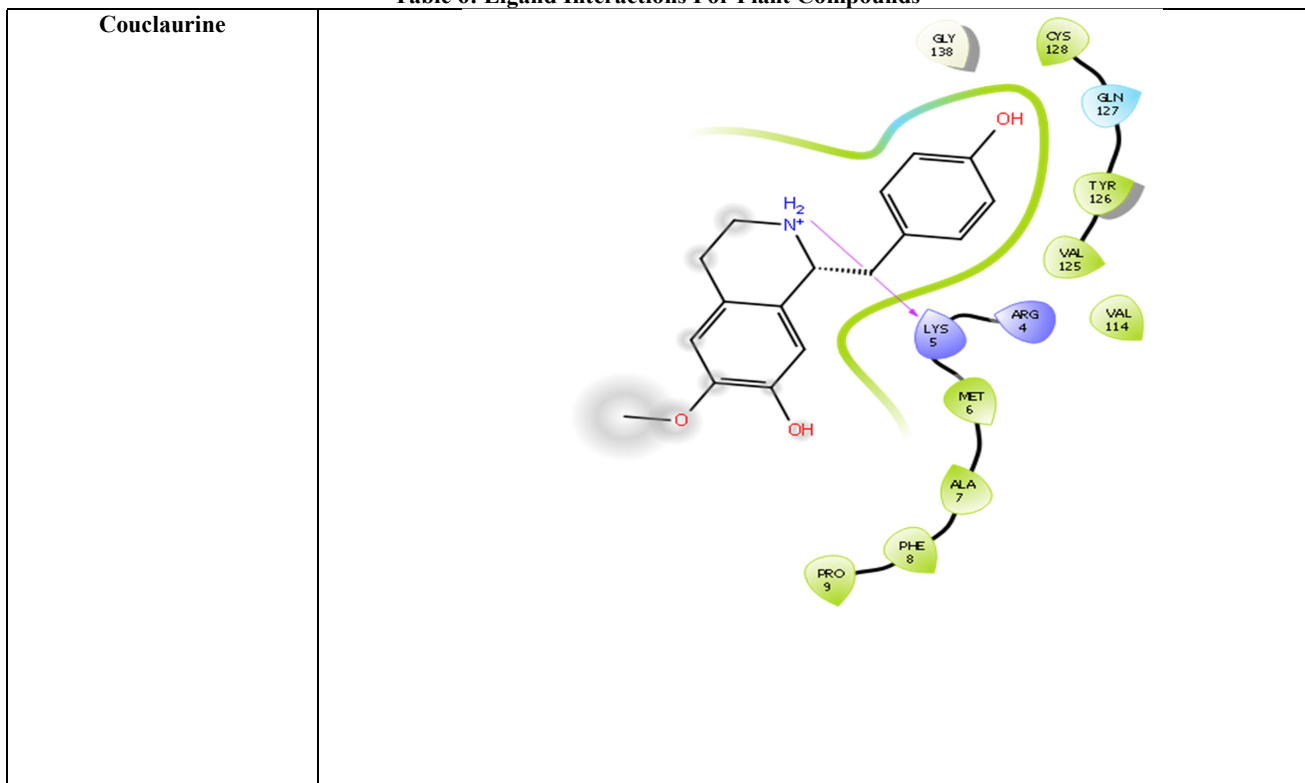
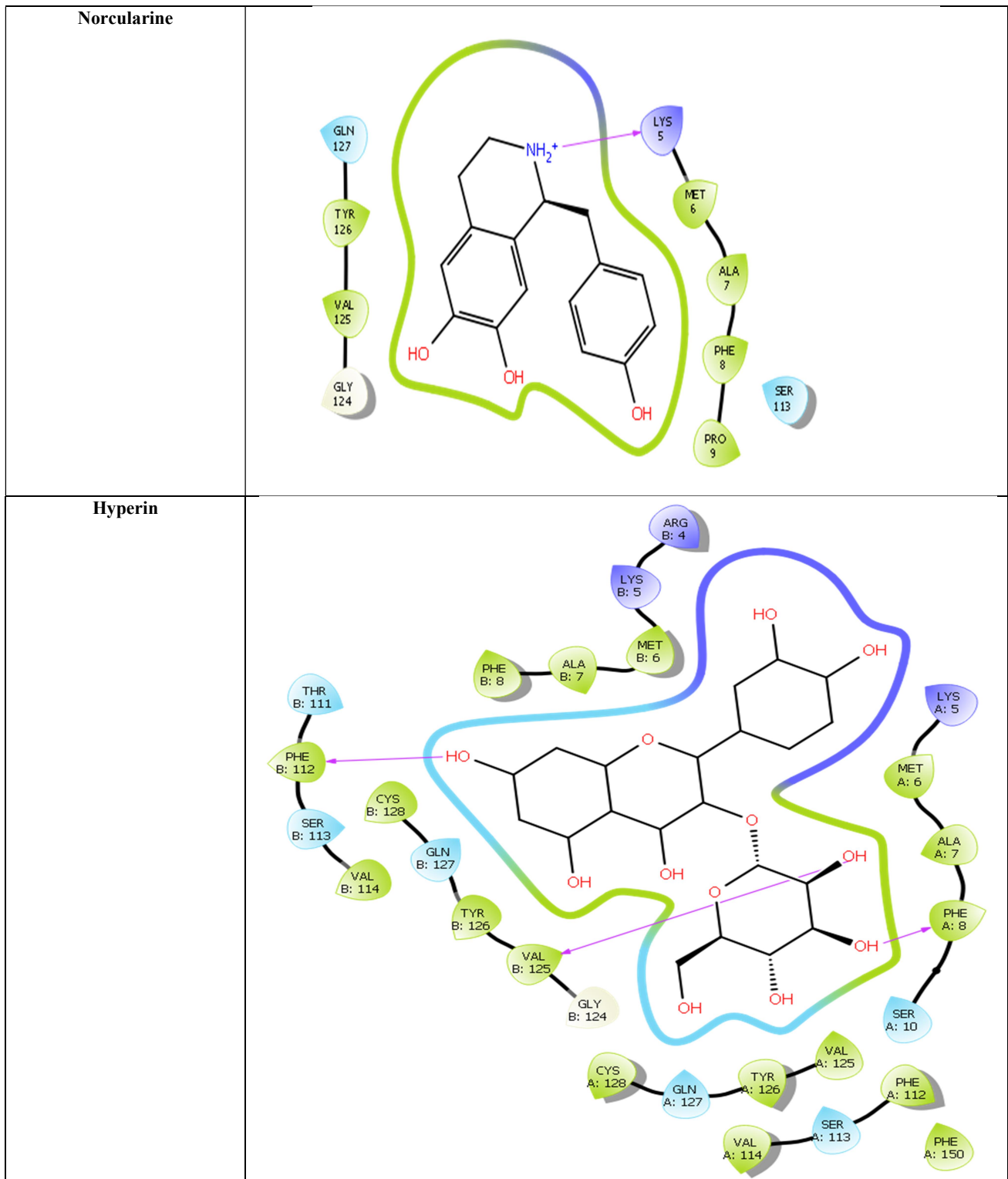


Table 6: Ligand Interactions For Plant Compounds





RESULT:

In the present work the molecular docking study of the data set of synthetic and plant was performed by Maestro version 11.5. The values of Synthetic and Natural compounds with respective binding energy are tabulated in **Table 3 & 4**. In this study we have used 5R82 as target. Molecular docking results displayed that compound (**P2**) showed the better docked score with better Antiviral and potency against COVID 19 as the interaction shown with 5R82 as amino acid with docking score **-6.01 Kcal/mol** with glide energy of **-38.883 Kcal/mol**. The compound P2 showed good properties within the close agreement of the Lipinski's rule of five and Qikprop rule within the range and thus making these compounds as suitable drug candidate [14]. The comparison of Synthetic and Plant compounds was depicted in graphical representation. (**Graph-1**), similarly the Ligand interactions are tabulated in **Table 4-6** for Synthetic and Plant compounds.

DISCUSSION

From the docking results among the Synthetic and Natural compounds docked with the protein 5R82, Compound P2 has shown greater binding energy, ligand efficiency and greater inhibition constant. The interactions with the enzyme protein and

ligand has shown greater binding energy. From the results on comparison of binding energy with synthetic and currently marketed drugs with that of natural compounds it is shown that natural compound P2 has shown more efficient binding energy prediction values.

CONCLUSION:

From the above results it's clear that the compound **P2** has possessed with greater binding energy values and has proven to be a greater efficiency against the inhibition of SARS COV 2(COVID-19) by insitu computational Docking Studies.

ACKNOWLEDGMENT:

The authors are thankful to Dr. M.G.R. Educational and Research Institute and its management for providing research facilities and encouragement. The authors are also thankful for Vinod Devaraji Senior Scientist, Schrodinger, Kishore V Associate Solutions Architect, Schrodinger for the support and throughout the project.

REFERENCES:

- [1] Cock, Ian & Cheesman, Matthew. (2016). Oceania: Antidepressant Medicinal Plants. 10.1007/978-3-319-14021-6_10.
- [2] Coclaurine from *Ocotea duckeida* Silva IG, Barbosa-Filho JM, da Silva

- MS, de Lacerda CD, da-Cunha EV *Biochem. Syst. Ecol.*, 2002
- [3] Bennett MR, Thompson ML, Shepherd SA, Dunstan MS, Herbert AJ, Smith DRM, Cronin VA, Menon BRK, Levy C, Micklefield J. Structure and Biocatalytic Scope of Coclaurine N-Methyltransferase. *Angew Chem Int Ed Engl.* 2018 Aug 13; 57(33): 10600-10604. doi: 10.1002/anie.201805060. Epub 2018 Jun 28. PMID: 29791083; PMCID: PMC6099451.
- [4] Sharma A, Tiwari S, Deb MK, Marty JL. Severe acute respiratory syndrome coronavirus-2 (SARS-CoV-2): a global pandemic and treatment strategies. *Int J Antimicrob Agents.* 2020; 56(2): 106054. doi:10.1016/j.ijantimicag.2020.106054
- [5] Shereen, Muhammad & Khan, Suliman & Kazmi, Abeer & Bashir, Nadia & Siddique, Rabeea. (2020). COVID-19 infection: Origin, transmission, and characteristics of human corona viruses. *Journal of Advanced Research.* 24. 10.1016/j.jare.2020.03.005.
- [6] Hemalatha C.N. *et al*; Reimpurposing of marketed drugs in treatment of COVID 19 by insilico methods . <https://doi.org/10.31838/ijpr/2020.SP1.337>
- [7] Driessche GVD, Fourches D (2017). Adverse drug reactions triggered by the common HLA-B*57:01 variant: a molecular docking study. *J Cheminform* 9(13): 1–17
- [8] Sastry GM, Adzhigirey M, Day T, Annabhimoju R, Sherman W (2013) Protein and ligand preparation: parameters, protocols and influence on virtual screening enrichments. *J Comput Aid Mol Des* 27(3): 221–234
- [9] .Kumar S, Singh J, Narasimhan B, Shah SAA, Lim SM, Ramasamy K, Mani V (2018) Reverse pharmacophore mapping and molecular docking studies for discovery of GTPaseHRas as promising drug target for bis-pyrimidine derivatives. *Chem Cent J* 12(106): 1–11
- [10] Sharma V, Sharma PC, Kumar V (2016) Insilico molecular docking analysis of natural pyridoacridines as anticancer agents. *Adv. Chem* 2016:1–9
- [11] Singh J, Kumar M, Mansuri R, Sahoo GC, Deep A (2016) Inhibitor designing, virtual screening and

docking studies for methyltransferase: a potential target against dengue virus. *J Pharm BioalliedSci* 8(3): 188–194

[12] Friesner RA, Murph RB, Repasky MP, Frye LL, Greenwood JR, Halgren TA, Sanschagrin PC, Mainz DT (2006) Extra precision glide: docking and scoring incorporating a model of hydrophobic enclosure for protein–ligand complexes. *J Med Chem* 49:6177–6196

[13] Lenselink EB, Louvel J, Forti AF, van Veldhoven JPD, de Vries H, MulderKrieger T, McRobb FM, Negri A, Goose J, Abel R, van Vlijmen HWT, Wang L, Harder E, Sherman W, IJzerman AP, Beuming T (2016) Predicting binding affinities for GPCR ligands using free-energy perturbation. *ACS Omega* 1: 293–304

[14] Tahlan, S., Kumar, S., Ramasamy, K. *et al.* In-silico molecular design of heterocyclic benzimidazole scaffolds as prospective anticancer agents. *BMC Chemistry* **13**, 90 (2019).
<https://doi.org/10.1186/s13065-019-0608-5>.